Multichannel interaction mechanism in a molecule-metal interface

Wei Ji,[1] Zhong-Yi Lu,[2] and Hong-Jun Gao[1]

[1]*Beijing National Laboratory for Condensed Matter Physics, Institute of Physics, Chinese Academy of Sciences,*
P.O. Box 603, Beijing 100080, China
[2]*Department of Physics, Renmin University of China, Beijing 100872, China*
(Received 15 February 2008; published 13 March 2008)

Using first-principles density functional theory calculations, we reveal that the nature of the PTCDA and Ag(111) interface is characterized by multichannel molecular orbital interactions. The interacting channels via the occupied electronic states are primarily located at the periphery of PTCDA, whereas those via the unoccupied states are at the center of PTCDA. Our theory provides a unified picture explaining all the exciting experiments. Also, a confined two-dimensional free-electron-like interface state is discussed.

The interaction mechanism between perylene-3,4,9,10-tetracarboxylic-3,4,9,10-dianhydride (PTCDA) and noble metal surfaces, e.g., Ag(111), has become one of the most fundamental issues in understanding molecular electronics and modeling of molecular self-assembly.[1–9] In spite of the intensive studies over the past ten years, the nature of this interface interaction remains unclear. There are two competing arguments which are under current debate. One school of thought considers the interface to be dominated by the bonding between the central benzene ring of PTCDA and the underneath Ag surface atoms, while the other considers the bonding between the terminal carboxylic O atoms and Ag atoms to be as important.

Most earlier experiments supported the notion of interaction via the central benzene ring. The electron photoemission spectroscopy observed significant energy shifts of the frontier orbitals located on the carbon ring (perylene core) but not the oxygen atoms of the anhydride groups,[2] indicating that the PTCDA binds to the surface through the perylene π system. Raman spectroscopy[3] showed an adsorption-induced peak shift from 1310 to 1297 cm^{-1},[3] which was assigned to be the shift of a breathing mode of the central benzene ring and its adjacent four hydrogens upon surface adsorption. High resolution electron energy loss spectroscopy[4] (HREELS) revealed significant enhancement of four vibrational modes by the substrate Ag surface, which was interpreted to be caused by the coupling of a dynamical dipole-induced electric field and the incident electrons, and the dynamical dipole was induced by the π-system-mediated charge "pumping" from the substrate to the central benzene ring.

However, a recent experiment by normal incident x-ray standing waves[9] (NIXSWs) has revealed a different interacting channel via the four terminal carboxylic O atoms bonding with the underneath Ag atoms, while the bonding between C and Ag did not appear. The discrepancy between this experiment and the earlier experiments was further compounded by the difference in theoretical calculations. One density functional theory (DFT) calculation showed a shift of benzene ring breathing mode in support of Raman experiment,[3] while another DFT calculation showed the covalent bonding between O and Ag but not between the benzene ring and the substrate.[8] However, this calculation produced a heavily bent perylene core, which disagrees with the NIXSW experiment. The failure of the earlier calculations has cast doubt on whether the DFT calculations can correctly describe such systems. Very recently, by including the electron core–hole interaction and its induced ionic relaxation in the DFT calculation, the x-ray photoemission spectroscopy and NIXSW experiments have been theoretically reproduced,[9] which indicates that the DFT method can describe such systems well if an appropriate physical picture is included.

It is puzzling why different experiments observed different interface interactions. Is it possible that both interacting channels coexist? And if so, which one is the primary interaction? To answer these questions, in this Brief Report, we report careful extensive DFT calculations to systematically investigate the interaction between PTCDA and Ag(111). We found that both interacting channels coexist in such a way that the O-Ag interaction acts at the periphery of the molecule via the occupied electronic states, while the C-Ag interaction acts at the center of the molecule (benzene ring) via the unoccupied states. Overall, the multichannel molecule-metal interaction involves multiple molecular orbitals at different surface regions. Our findings provide a unified physical picture explaining all the experiments. Those early experiments see only the C-Ag interaction mode because they are all excited-state spectroscopies sensitive to the unoccupied states, while the NIXSW experiment sees the O-Ag interaction because it reflects ground-state structure properties sensitive to the occupied states. Furthermore, it also allowed us to understand the origin of the observed free-electron-like behavior.[11]

Partial details (calculation setups) of ground-state calculations were described in a previous publication.[9] To make the interaction clearer, we first studied the system with a single PTCDA adsorbed on Ag(111). With respect to the two-dimensional (2D) layer projected density of states (LPDOS), the full monolayer model was adopted. The Raman frequency analysis was done using the GAUSSIAN03 package[13] at the B3LYP/6-31G* level, double checked at the B3PW91/6-31G* and LSDA-SVWN/6-31G* levels. The structures for frequency analysis were supplied by taking the PTCDA away from the fully relaxed adsorbed structures.

We first analyze the differential charge density (DCD) of the PTCDA-Ag(111) system. The DCD here is defined as $\rho_{DCD} = \rho_{total} - \rho_{PTCDA} - \rho_{Ag(111)}$, which directly reveals the in-
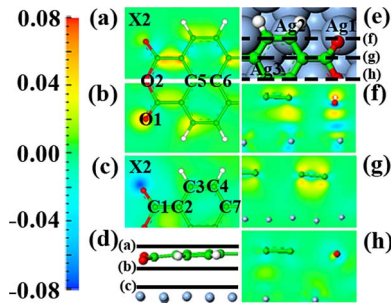
FIG. 1. (Color online) [(a)–(c)] Top views of DCDs of a PTCDA adsorbed on Ag(111) on planes at different heights shown by (d). [(f)–(h)] Side views. (d) Side view and (e) top view of the real-space models indicating three plane positions in the top views [(a)–(c)] and side views [(f)–(h)] of DCDs. The "×2" means that the densities are scaled by a factor of 2.

formation on adsorption-induced chemical bond formation. Figures 1(a)–1(c) show the calculated DCDs of PTCDA adsorbed on Ag(111) at three different heights. One can see a definite charge transfer from the substrate to the PTCDA. The real-space distribution of DCD in Fig. 1(a) is similar to that of the bare PTCDA's lowest unoccupied molecular orbital (LUMO). This suggests that the adsorption-induced net charge transfer is highly related to the LUMO of PTCDA. To facilitate our discussion, we denote two kinds of O atoms (O1 and O2), seven kinds of C atoms (C1 to C7), and three kinds of Ag atoms (Ag1 to Ag3), as shown in Fig. 1. Because of the small distance between O1 and its underneath Ag1, a covalent bond between them was suggested in a previous work.[8] As expected, at the height near the substrate surface [Fig. 1(c)], a significant charge reduction just above Ag1 is obtained. This reduction reflects that a covalentlike bond formed between O1 and Ag1. To our surprise, the DCD at the height just below the molecule [Fig. 1(b)] shows only two pointlike enhancement at O1 and C3. Another relatively weak and delocalized enhancement is found around the C1 and C2, which likely results from the conjugated effect of O1 (to C2) and C3 (to C1).[14] We notice that the transferred charge at the central benzene ring in Fig. 1(a) is absent in Fig. 1(c). To further understand the bonding mechanism, we also plot the side views of DCD at three cross-section planes [denoted in Fig. 1(e)], as shown, respectively, in Figs. 1(f)–1(h). They clearly indicate that there are only two definite bonds that formed between PTCDA and Ag(111), i.e., the O1-Ag1 bond and a C3-Ag2 bond, which explains the enhanced spots around C3 in the previous scanning tunneling microscopy experiments.[12] Differing from the O1-Ag1 bond,

the weaker and more delocalized characteristic is observed in the C3-Ag2 bond.

Before further analyzing the bonding mechanism, we calculated the energy levels of a free standing PTCDA's molecular orbitals (MOs), as shown in Table I. In order to subsequently analyze the electronic hybridization, we align the calculated highest occupied molecular orbital (HOMO) to the measured value of −2.2 eV.[10,14] All levels are shifted according to this alignment (same in all the discussions below). Moreover, the unoccupied states are calibrated by the experimental HOMO-LUMO gap of 2.3 eV.[14,15] Table I shows that in the energy window from −4.0 to 0.0 eV, there are three sets of orbitals. The first set contains six orbitals, i.e., HOMO-8 to HOMO-3 from −3.74 to −3.49 eV (−3.68 to −3.44 eV for GGA-PBE), which are four π-like and two in-plane σ-like MOs, respectively. The second set of MOs contains HOMO-2 and HOMO-1 around −2.9 eV. They are also in-plane σ MOs. The third one is the HOMO. By scaling[14] the unoccupied states, we have assigned the levels of 0.1 and 2.2 eV to be the LUMO and the LUMO +1, respectively.

We now analyze the projected density of states (PDOS) of PTCDA adsorbed on Ag(111). The results are summarized in Table II. In the relevant energy window from −3.0 to 2.0 eV, there are five separate sets of states denoted as S1 to S5, respectively. The S1 set, from −2.60 to −2.47 eV, corresponds to the observed very broad ultraviolet photoemission spectroscopy (UPS) peak from −3.5 to −2.5 eV. This broad peak contains at least four to five states that cannot be distinguished experimentally.[10] The previous study regarded this peak as the hybrid bonding states of HOMO and Ag d band.[10] However, inspection of the calculated HOMO position of −2.2 eV and the calculated d band upper edge at −3.6 eV [experimentally below −4 eV (Ref. 10)] reveals that these states cannot be the bonding state of HOMO and d states. The reason is that, in electronic hybridization, it is impossible to have a bonding state higher in energy than each of its components, e.g., Ag d band or PTCDA's HOMO here. In comparison with a freestanding PTCDA (Table I), a few MOs, e.g., from H-8 to H-3, are at −3.74 to −3.49 eV. From the energetic point of view, the S1 states should be the antibonding states of these MOs, being confirmed by a real-space charge density plot.[14] The H-2 and H-1, two in-plane σ MOs, are at −2.98 and −2.88 eV. Their energy levels are hardly shifted by the interaction between PTCDA and Ag(111). Thus, they may contribute to the broad peak from −3.5 to −2.5 eV in the UPS data,[10] too.

Regarding the hybridization of HOMOs and LUMOs, respectively, with the substrate states, the UPS study[10] showed

TABLE I. Calculated [DFT-LDA/GGA(PBE)] and calibrated (LDA/GGA-Ca) (Ref. 14) values (in eV) of a freestanding PTCDA's MOs. The H and L mean the HOMO and the LUMO of PTCDA, respectively.

Levels	H-8 to H-3	H-2/H-1	H	L	L+1
DFT-LDA	−3.74 to −3.49	−2.89/−2.88	−2.20	−0.69	0.68
LDA-Ca				0.1	2.19
DFT-GGA	−3.68 to −3.44	−2.96/2.95	−2.20	−0.70	0.65
GGA-Ca				0.1	2.15

TABLE II. Five sets of the relevant states and their energy levels versus the Fermi energy ("Level"), the two hybrid components ("Mol" for PTCDA and "Sub" for substrate), the UPS, and the STS measurements of the corresponding states in the energy windows from −3.0 to 2.0 eV. The n in L+n means that there are a few MOs from L+1 involved in the S5.

	S1	S2	S3	S4	S5
Level	−2.60 to −2.47	−1.64/−1.52	−0.53	0.20–0.32	0.49–2.0
Mol	H-8 to H-1	H	L	L	L+n
Sub	d	d	$p(s)$	$p(s)$	$p(s)$
UPS (Ref. [10])	−3.5 to −2.5	−1.6	−0.3		
STS (Ref. [11] and [12])		−1.7	−0.3		0.7

two peaks at −1.6 and −0.3 eV, while a recent scanning tunneling spectroscopic (STS) measurement[12] suggested −1.7 and −0.3 eV. Our calculation shows that the HOMO-d hybrid antibonding state splits into two states, respectively, at −1.64 and −1.52 eV (S2), while a LUMO-$p(s)$ hybrid bonding state exists at −0.53 eV (S3) [the monolayer model gives this value of roughly −0.3 eV, see Fig. 3(a)]. The real-space charge density plots of these states (S2 and S3) further show the PTCDA-Ag(111) interaction through O1-Ag1 and C3-Ag2 channels.[14] Consistent with our previous work,[9] the S4 set is the hybrid antibonding state by LUMO and Ag $p(s)$ states, which is very close to its bonding state in energy. From the electronic hybridization point of view, the S5 states, from 0.49 eV to the end of our energy window, are hybrid bonding states Ag $p(s)$ states and some of the unoccupied states, e.g., LUMO+1 [LUMO+n (Ref. [14])]. According to Fig. 2, the state (S5a) at 0.70 eV, which has the largest intensity in S5, as shown in Fig. 3(a), is a bonding state formed by LUMO+1 and Ag $p(s)$ states. Meanwhile, the second largest state in S5 (S5b) is found roughly at 1.7 eV. In comparison with the STS measured values of roughly 0.7 and 1.6 eV, both calculated states (S5a and S5b) are highly consistent with the STS measurements.[11] In particular, the PDOS of S5a shows the p characteristics from all the relevant Ag atoms, e.g., Ag1 to Ag3.[14] Furthermore, Fig. 2(left) clearly shows the nature of an interface state (S5a) confined in between the molecule and the substrate, with a 2D quantum-well-like behavior. The interacting channels are available over the entire molecule, e.g., C6-Ag3 [the strongest, see Fig. 2(right)], O1-Ag1, and C3-Ag2 channels.[14]

For a PTCDA monolayer on Ag(111), we define the LP-DOS as the DOS projected into planes parallel to the surface at different heights. In the calculation, we integrated the atomically decomposed DOS of the first layer Ag atoms and all the atoms in PTCDA to obtain the LPDOS. Figure 3(a) displays the calculated LPDOS of a monolayer PTCDA on Ag(111) in comparison with the one [Fig. 3(b)] for a single PTCDA on Ag(111). One can see from Fig. 3 that the S3 and S4 states broaden into a wide band crossing the Fermi Level in the monolayer case, while the S5 state broadens into a band as well, being highly consistent with previous experimental data.[11,12] Especially, the relatively flat S5 LPDOSs indicate that the band formed by the S5 states behaves as a 2D free electron. The underlying physics is that the LUMOs and LUMO+n's of neighbor PTCDAs, although no chemical bonds form between them, effectively overlap, respectively, mediated by the extended substrate $s(p)$ states hybridizing with the LUMOs and LUMO+n's. Here, the scenario is similar to the Ruderman-Kittel-Kasuya-Yosida interaction between magnetic impurities embedded in a nonmagnetic metal. It turns out that the electrons in different PTCDA molecules in monolayer coverage can talk to each other, mediated by those states of S3 and/or S4 around the Fermi energy rather than directly or via the terminal O-Ag covalent bonds or possible C-H⋯O hydrogen bonds. This is consistent with a recent STS measurement,[11] which suggested that the direct electronic coupling between PTCDA molecules is much smaller than the substrate-mediated coupling.
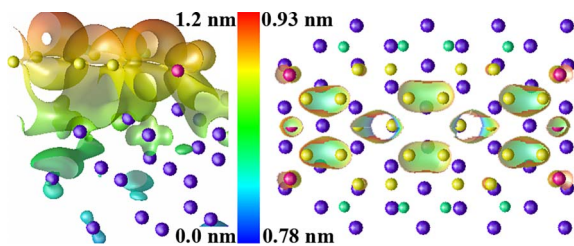

FIG. 2. (Color online) Side view (left) and top view (right) of the real-space density of the largest state in S5 at 0.70 eV above the Fermi energy. The color of the isosurface is mapped by z values in the supercell. Two holes on the isosurface can be found around C6 atoms.
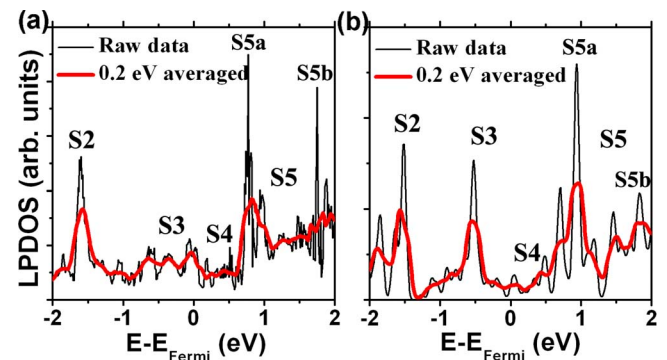

FIG. 3. (Color online) Layer projected density of states of the molecule-substrate interface for (a) monolayer PTCDA and (b) single PTCDA on Ag(111). The black thin lines represent the raw data and the red thick lines yield the average with a resolution of 0.2 eV.

In a HREELS experiment, only the valence charges are involved in forming the dynamical dipole-induced electric field. This means that the charge pumping channels are among our obtained interacting channels, i.e., O1-Ag1, C3-Ag2, and C6-Ag3. In general, the surface enhanced Raman scattering (SERS) in the EELS experiment is mostly due to the incidence electron induced surface plasma. When an incidence electron in EELS approaches the surface, it can either be trapped by the surface, forming sample current, or be impacted by the surface, contributing to the EELS signal. If an electron with 2.5 eV kinetic energy, as described in previous HREELS experiments,[4] is injected into the surface, it cannot excite the surface plasma of Ag(111) since the threshold energy of this plasma is roughly equal to 3.8 eV.[16] However, in a particular case of 2D nanometer-scale free electron gas, the plasma can be excited by very low incidence electron energy, e.g., tens of meV.[16] The electron of 2.5 eV in energy can definitely excite the plasma of such a 2D state, i.e., the confined 2D free-electron-like S5 state here. The experimentally observed SERS by HREELS was shown to be related to the central benzene ring of PTCDA.[4] Here, we show that the strongest interacting channel set by S5 is through C6-Ag3 around the central benzene ring. Therefore, the excited 2D plasma of S5, confined between PTCDA and Ag(111), is very likely responsible for inducing the SERS.

Generally, the structural deformation could shift the vibrational frequencies of molecules on surfaces. For the same reason, the bent molecular backbone of PTCDA adsorbed on Ag(111) may correspond to the observed Raman shift, from 1310 to 1297 cm^{-1},[3] of the central benzene ring. For a flat PTCDA, the frequency of this Raman mode was calculated as 1324 cm^{-1}, while the bent one gives two modes, at 1265 and 1292 cm^{-1}. In comparison, the calculated shift is well consistent with the experimental one. The calculations using different functionals do not change the value of this shift significantly.

In summary, we show that the PTCDA-Ag(111) interaction is a multichannel one. A number of MOs, at least from HOMO-8 to LUMO+1, are involved in the molecule-metal bonding. Both the d band and the $p(s)$ band of the Ag substrate are involved as well. The primary interacting channels are O1-Ag1 and C3-Ag2 (at the corner of PTCDA) for the occupied states and C6-Ag3 (around the center of PTCDA) for the unoccupied states. Based on this picture, a unified and comprehensive understanding of the interaction mechanism is achieved. The observed confined interface state (S5) may open a new area concerning the 2D free electron gas confined in the molecule-metal interface. The multipoint characteristic of this interaction, which may result in multiple metastable configurations, is expected as a general behavior of molecule-metal bonding. These metastable configurations can be achieved by the lateral influence in the monolayer, e.g., the lateral alkyl chains.[17] This makes organic molecules good prototypes for the demonstration of structural modulation or for achieving selective molecular recognition in metal-organic hybrid systems.[8]

[1] Jordi Fraxedas, *Molecular Organic Materials* (Cambridge University Press, Cambridge, 2006) and references therein.

[2] E. Umbach, C. Seidel, J. Taborski, R. Li, and A. Soukopp, Phys. Status Solidi B **192**, 389 (1995); E. Umbach, M. Sokolowski, and R. Fink, Appl. Phys. A: Mater. Sci. Process. **63**, 565 (1996).

[3] V. Wagner, Phys. Status Solidi A **188**, 1297 (2001).

[4] M. Eremtchenko, J. A. Schaefer, and F. S. Tautz, Nature (London) **425**, 602 (2003).

[5] A. Hauschild, K. Karki, B. C. C. Cowie, M. Rohlfing, F. S. Tautz, and M. Sokolowski, Phys. Rev. Lett. **94**, 036106 (2005).

[6] R. Rurali, N. Lorente, and P. Ordejón, Phys. Rev. Lett. **95**, 209601 (2005).

[7] A. Hauschild, K. Karki, B. C. C. Cowie, M. Rohlfing, F. S. Tautz, and M. Sokolowski, Phys. Rev. Lett. **95**, 209602 (2005).

[8] S. X. Du, H. J. Gao, C. Seidel, L. Tsetseris, W. Ji, H. Kopf, L. F. Chi, H. Fuchs, S. J. Pennycook, and S. T. Pantelides, Phys. Rev. Lett. **97**, 156105 (2006).

[9] W. Ji, Z.-Y. Lu, and H. J. Gao, Phys. Rev. Lett. **97**, 246101 (2006).

[10] Y. Zou, L. Kilian, A. Schöll, Th. Schmidt, R. Fink, and E. Umbach, Surf. Sci. **600**, 1240 (2006).

[11] R. Temirov, S. Soubatch, A. Luican, and F. S. Tautz, Nature (London) **444**, 350 (2006).

[12] A. Kraft, R. Temirov, S. K. M. Henze, S. Soubatch, M. Rohlfing, and F. S. Tautz, Phys. Rev. B **74**, 041402(R) (2006).

[13] M. J. Frisch *et al.*, GAUSSIAN 03, Revision C.02, Gaussian, Inc., Wallingford, CT, 2004.

[14] See EPAPS Document No. E-PRBMDO-77-086811 for the details of a few terms, figures, tables, states, and channels. For more information on EPAPS, see http://www.aip.org/pubservs/epaps.html.

[15] H. Proehl, T. Dienel, R. Nitsche, and T. Fritz, Phys. Rev. Lett. **93**, 097403 (2004).

[16] M. Rocca, Surf. Sci. Rep. **22**, 1 (1995).

[17] D. X. Shi *et al.*, Phys. Rev. Lett. **96**, 226101 (2006).